JPn Neuroscience

The Journal of Physiology

J Physiol 591.22 (2013) pp 5509–5523

Burst generation mediated by cholinergic input in terminal nerve-gonadotrophin releasing hormone neurones of the goldfish

Takafumi Kawai[1,2], Hideki Abe[1,3] and Yoshitaka Oka[1]

[1] *Department of Biological Sciences, Graduate School of Science, The University of Tokyo, 7-3-1 Hongo, Bunkyo-ku, Tokyo 113-0033, Japan*
[2] *Integrative Physiology, Graduate School of Medicine, Osaka University, Yamada-oka 2-2, Suita, Osaka 565-0871, Japan*
[3] *Laboratory of Fish Biology, Graduate School of Bioagricultural Sciences, Nagoya University, Furo-cho, Chikusa-ku, Nagoya 464-8601, Japan*

Key points

- Burst firing activities are effective for the release of neuropeptides from peptidergic neurones.
- A peptidergic neurone, the terminal nerve (TN)-gonadotrophin releasing hormone (GnRH) neurone, shows spontaneous burst firing activities only infrequently.
- Only a single pulse electrical stimulation of the neuropil surrounding the TN-GnRH neurones induces transient burst activities in TN-GnRH neurones via cholinergic mechanisms.
- The activation of muscarinic acetylcholine receptors results in a long-lasting hyperpolarisation, inducing rebound burst activities in TN-GnRH neurones.
- These new findings suggest a novel type of cholinergic regulation of burst activities in peptidergic neurones, which should contribute to the release of neuropeptides.

Abstract Peptidergic neurones play a pivotal role in the neuromodulation of widespread areas in the nervous system. Generally, it has been accepted that the peptide release from these neurones is regulated by their firing activities. The terminal nerve (TN)-gonadotrophin releasing hormone (GnRH) neurones, which are one of the well-studied peptidergic neurones in vertebrate brains, are characterised by their spontaneous regular pacemaker activities, and GnRH has been suggested to modulate the sensory responsiveness of animals. Although many peptidergic neurones are known to exhibit burst firing activities when they release the peptides, TN-GnRH neurones show spontaneous burst firing activities only infrequently. Thus, it remains to be elucidated whether the TN-GnRH neurones show burst activities and, if so, how the mode switching between the regular pacemaking and bursting modes is regulated in these neurones. In this study, we found that only a single pulse electrical stimulation of the neuropil surrounding the TN-GnRH neurones reproducibly induces transient burst activities in TN-GnRH neurones. Our combined physiological and morphological data suggest that this phenomenon occurs following slow inhibitory postsynaptic potentials mediated by cholinergic terminals surrounding the TN-GnRH neurones. We also found that the activation of muscarinic acetylcholine receptors induces persistent opening of potassium channels, resulting in a long-lasting hyperpolarisation. This long hyperpolarisation induces sustained rebound depolarisation that has been suggested to be generated by a combination of persistent voltage-gated Na^+ channels and low-voltage-activated Ca^{2+} channels.

DOI: 10.1113/jphysiol.2013.258343

These new findings suggest a novel type of cholinergic regulation of burst activities in peptidergic neurones, which should contribute to the release of neuropeptides.

(Received 18 May 2013; accepted after revision 16 August 2013; first published online 19 August 2013)
Corresponding author Y. Oka: Department of Biological Sciences, Graduate School of Science, The University of Tokyo, 7-3-1 Hongo, Bunkyo-ku, Tokyo 113-0033, Japan. Email: okay@biol.s.u-tokyo.ac.jp

Abbreviations Ach, acetylcholine; ChAT, choline acetyltransferase; GIRK channel, G protein-coupled inwardly rectifying potassium channel; GnRH, gonadotrophin releasing hormone; IPSC, inhibitory postsynaptic current; IPSP, inhibitory postsynaptic potential; LVA, low-voltage-activated; mAchR, muscarinic acetylcholine receptor; MAP, microtubule-associated protein; NMDG, *N*-methyl-D-glucamine; PBS, phosphate-buffered saline; PSTH, peristimulus time histogram; TN, terminal nerve; TTX, tetrodotoxin; VGCC, voltage-gated calcium channel; VGSC, voltage-gated sodium channel.

Introduction

Peptidergic neurones play important roles in the modulation of neuronal activities in various brain regions (Leng & Ludwig, 2006). Neuropeptides released from these neurones are reported to diffuse and affect distant targets; e.g. they have been reported to modulate the firing activities, synaptic transmission and signal transduction of neurones in widespread regions of the nervous system (Jan & Jan, 1983; Leng & Ludwig, 2006). Although the classical neurotransmitters, such as glutamate and GABA, are packaged in small clear synaptic vesicles and are released at synaptic active zones, the neuropeptides are packaged in large dense-core vesicles (Whitnall & Gainer, 1985; Oka & Ichikawa, 1991, 1992; Salio *et al.* 2006) and have been suggested to be released non-synaptically from the somatodendritic area and axons (Oka & Ichikawa, 1991, 1992; Castel *et al.* 1996; Ludwig & Leng, 2006). Although the relationship between the electrical activity of the single peptidergic neurone and the release of neuropeptide has not been studied systematically, the release of neuropeptide has been reported to be evoked by high-frequency firing, such as burst firing (Dutton & Dyball, 1979; Ishizaki *et al.* 2004; Liu *et al.* 2011).

The terminal nerve (TN)-gonadotrophin releasing hormone (GnRH) peptidergic neurones are one of the well-studied central peptidergic neurones, as their large cell bodies form characteristic clusters in close association with the olfactory bulb and are easily identified morphologically throughout vertebrates, including mammals (Oka & Ichikawa, 1990; Kim *et al.* 1995; Kim *et al.* 1999). They project their axons to wide brain regions and have been suggested to function as important regulators of sensory responsiveness of animals in response to their environments (Eisthen *et al.* 2000; Yamamoto & Ito, 2000; Park & Eisthen, 2003; Kinoshita *et al.* 2007; Kawai *et al.* 2009, 2010; Maruska & Tricas, 2011). They usually show spontaneous and intrinsic tonic regular firing activities (pacemaker activity), whose firing frequency can be regulated by constant current injection or by modifying the K^+ concentration of the external solution (Oka & Matsushima, 1993; Ishizaki *et al.* 2004). The ionic mechanisms of spontaneous firing and the basic ionic channel properties of the TN-GnRH neurones have already been well studied using teleost brain preparations because of their experimental advantages, such as the large cell size and ease of stable electrical recording (Oka & Matsushima, 1993; Oka, 1996; Abe & Oka, 1999). These previous studies have suggested that the release of GnRH peptides measured by radioimmunoassay is well correlated to the firing frequency of TN-GnRH neurones, and high-frequency firings of these neurones are important for GnRH release in the brain (Ishizaki *et al.* 2004). Thus, the TN-GnRH neurone is considered to be an excellent model neurone for the study of the relationship between the electrical activity and release of neuropeptides.

In this study, we found that TN-GnRH neurones can exhibit a transient burst firing after a long-lasting slow inhibitory postsynaptic potential (IPSP) that is induced by a single pulse stimulation of fibres around the TN-GnRH neurones. This slow IPSP has been suggested to be caused by the stimulation of cholinergic fibres around the TN-GnRH neurones and to elicit rebound burst activity. From these results, we suggest a novel type of long-lasting strong cholinergic inhibition that evokes rebound burst activities in peptidergic neurones. It is possible that a similar mechanism may also work in other peptidergic neurones for the release of their neuropeptides.

Methods

Adult goldfish (*Carassius auratus*) were purchased from a local dealer in Tokyo and Nagoya. They were kept in 60 litter aquaria containing approximately 15 fish at room temperature before use for the experiments. A total of 100 fish was used in this study. All procedures were performed in accordance with the guiding principles for the care and use of animals in the field of physiological sciences (2003) by the Physiological Society of Japan and the University of Tokyo for the Use and Care of Experimental Animals. They also conformed with *The Journal of Physiology* standards (Drummond, 2009).

Preparation of TN-GnRH neurones

After the animals were anaesthetised on ice and decapitated, the whole brain was dissected out. The brain was immersed in a standard external solution containing (in mM) 150 NaCl, 3.0 KCl, 1.3 $MgCl_2$, 2.4 $CaCl_2$, 10 Hepes and 10 glucose (adjusted to pH 7.4 with NaOH). After the meningeal membrane covering the olfactory bulb had been carefully removed, the preparations were transferred to a recording chamber filled with standard external solution. As the TN neurones are located in the rostral surface of the olfactory bulb as a cluster, they could be clearly identified by their large size (more than 20 μm in diameter) under an upright microscope with infrared differential interference contrast optics (Fujita *et al.* 1985; Oka & Matsushima, 1993; Kim *et al.* 1995; Haneda & Oka, 2008).

Whole cell recordings from TN-GnRH neurones

Whole cell patch-clamp recordings were performed as follows. Recording pipettes were made of borosilicate glass (G-1.5; Narishige, Tokyo, Japan) using a puller (P-97; Sutter Instruments, Navato, CA, USA). We used KCl-based pipette solution, consisting of (in mM) 120 KCl, 3 $MgCl_2$, 40 Hepes, 0.3 EGTA, 2 Mg-ATP and 0.3 GTP (adjusted to pH 7.2 with KOH). The liquid junction potential between the standard external solution and the pipette solution was 3.7 mV and was not corrected. The pipettes had resistances of 1.0–4.0 MΩ. Whole cell recordings were performed using an Axopatch 200B, and electrical signals were low-pass filtered at 2 kHz and sampled at 5 kHz using Digidata 1322A and pCLAMP9.2 software (Molecular Devices, Foster City, CA, USA). The input resistance and membrane capacitance of these neurones measured 229.8 ± 40.9 MΩ and 131.2 ± 45.9 pF, respectively ($n = 9$). The resting membrane potential of these neurones was −53.2 ± 1.9 mV ($n = 9$), when it was defined as the trough of the regular spontaneous action potential activities, because all the recordings from TN-GnRH neurones showed such spontaneous activities; therefore, the measurement of the true 'resting' membrane potentials was difficult. For Na^+-free experiments, NaCl in external standard solution was replaced by equivalent *N*-methyl-D-glucamine (NMDG).

Electrical stimulation

A bipolar tungsten stimulus electrode, (TOG 210–064; Unique Medical, Tokyo, Japan; exposed length, 50 μm; inter-electrode distance, 100 μm) was positioned on the olfactory nerve, which is adjacent to the TN-GnRH neurones. The electrical stimuli (0.1–0.2 ms pulses at 0.5–1.0 mA) were delivered every 30 s using an electronic stimulator (SEN-3201; Nihon Kohden, Tokyo, Japan) through an isolation unit (SS-302J; Nihon Kohden).

Drug applications

Tetrodotoxin (TTX) and scopolamine hydrobromide n-hydrate [muscarinic acetylcholine receptor (mAchR) antagonist] were obtained from Wako (Tokyo, Japan). Acetylcholine (Ach) chloride, NMDG and gallamine triethiodide (mAchR antagonist) were purchased from Sigma (St Louis, MO, USA). Tertiapin-Q was purchased from Abcam (Cambridge, MA, USA). Both bath and puffer applications of the drugs were used. Ach was applied by puffer application using a solenoid valve controlled by Digidata 1322A (∼20 ms puff, 100–200 kPa). The other drugs were applied by bath application.

Analyses

We analysed the electrophysiological data with Clampfit 9.2 (Molecular Devices) and Igor Pro 6.22A (WaveMetrics, Portland, OR, USA). Spike detection and drawing of peristimulus time histograms (PSTHs) were performed using TaroTools (a plugin macro for Igor Pro) by Dr T. Ishikawa (Jikei Medical School, Tokyo, Japan). To determine the amplitude of slow IPSP, we set the most hyperpolarised value of the action potentials in TN-GnRH neurones as the baseline. The duration was determined by measuring the interval between the start time of the hyperpolarisation and the time at which the hyperpolarised membrane potential recovered to the baseline.

Statistical analyses were performed with Kyplot software (version 3; Kyence, Tokyo, Japan). For two-group comparison (Fig. 5*C*), we first examined whether it met the equal variance conditions for every analysis. If so, we used Student's unpaired *t* test for statistics and, if not, Aspin–Welch *t* test. All the data in this study are represented as means ± SEM. For the multiple comparisons (Figs 2*G* and 6*B*), we performed Dunnett's test.

Immunohistochemistry

After the animals had been anaesthetised in 0.02% MS-222, they were perfused from the heart with 0.75% NaC1, followed by 4% paraformaldehyde in 0.1 M phosphate-buffered saline (PBS). The olfactory bulb was then fixed in the same fixative overnight at 4°C and washed with PBS (3 × 10 min). Nonspecific adsorption was blocked with 4% bovine serum albumin in PBS with Triton X-100 (0.1%) for 3 h at 37°C, and the fixed olfactory bulbs were reacted with primary antibodies for 24 h at 4°C. For immunohistochemistry, we used a combination of rabbit antiserum against choline acetyltransferase (ChAT) (dilution 1 : 500; anti-ChAT;

made by Johnson & Epstein, 1986) and a monoclonal mouse IgG against microtubule-associated protein (MAP) 2 (dilution 1 : 500; monoclonal anti-MAP2 (2a + 2b), clone AP-20, cat no. M1406; Sigma) in 2% bovine serum albumin in PBS with Triton X-100 (0.1%). After removal of the primary antibody by washing with PBS three times, the tissue was reacted with secondary antibody for 24 h at 4°C using biotinylated anti-rabbit IgG (1 : 500; Vector Laboratories, Burlingame, CA, USA) and Alexa555-conjugated anti-mouse IgG (1 : 500; Invitrogen, Carlsbad, CA, USA). The tissue was then incubated in a mixture of Vectastain Elite ABC kit (Vector Laboratories) and Alexa488-conjugated streptoavidin (1 : 100; Invitrogen, Carlsbad, CA, USA). After rinsing with PBS three times, the labelled olfactory bulbs were mounted in glycerol with 1,4-diazabicyclo[2,2,2]octane (i.e. anti-fading reagent) in 10 mM Tris–HCl (pH 8.0). A Zeiss LSM510 confocal laser scanning system (Carl Zeiss, Oberkochen, Germany) was used for collection of the fluorescence images. The digitised images were brightness and contrast adjusted by ImageJ software (Abramoff *et al.* 2004), and superimpose and three-dimensional reconstruction analysis of double fluorescence data was performed by Fluorender (Wan *et al.* 2009).

Results

Rebound burst activities following slow IPSPs

As has been reported previously (Oka & Matsushima, 1993; Wayne *et al.* 2005), the TN-GnRH neurones showed regular pacemaker activity with a firing frequency of 5.97 ± 1.32 Hz in the whole cell recording ($n = 9$). A single pulse electrical stimulation to the olfactory nerve fibres around the recording neurones (Fig. 1*A*) reproducibly caused a transient abolishment of pacemaker activity of TN-GnRH neurones immediately after the stimulation (Fig. 1*B–D*). The stimulation of TN-surround fibres induced slow IPSPs in the TN-GnRH neurones, whose latency and duration were 29.6 ± 2.42 ms (22.0–45.1 ms) and 474.0 ± 56.2 ms (335.0–889.2 ms), respectively ($n = 9$). The slow IPSP hyperpolarised the TN-GnRH neurones to -79.0 ± 2.07 mV, and the amplitude of slow IPSP was -25.5 ± 1.40 mV ($n = 9$) on average. After the slow IPSP, all TN-GnRH neurones also exhibited a transient burst firing activity (we name it 'the rebound burst activity' in this article; the maximum instantaneous firing rate was 37.5 ± 8.90 Hz) that lasted for more than 5 s. The slow IPSP was abolished by a bath application of TTX (0.75 μM; Fig. 1*E*), suggesting that this phenomenon is mediated by synaptic activity. A similar phenomenon was also induced in cell-attached loose-patch recordings (Fig. S1).

Next, we applied a square pulse current injection (1 s; 0.3–0.6 nA) to the TN-GnRH neurone, which can hyperpolarise the neurone by more than 20 mV, to examine whether the burst activities following slow IPSPs are mediated simply by strong hyperpolarisations in the TN-GnRH neurones (Fig. 1*F*). Similar to the slow IPSP, strong hyperpolarisation by current injection induced long-lasting burst activities of TN-GnRH neurones (Fig. 1*G–I*, $n = 4$). Taken together, these results suggest that the increase in firing activity observed after the slow IPSP is attributable to the endogenous channel properties of TN-GnRH neurones.

Slow IPSP is induced by the activation of mAchRs

In order to elucidate possible mechanisms for the generation of the slow IPSP, we first searched for a candidate neurotransmitter that is released to the TN-GnRH neurones after electrical stimulation of the TN-surround fibres, using various pharmacological agents (e.g. antagonists for GnRH receptors, neuropeptide FF receptors, dopamine receptors, metabotropic glutamate receptors, etc.) to see whether they blocked the generation of slow IPSPs. We found that a prior bath application of gallamine, an mAchR antagonist, affected slow IPSP. In the current clamp mode, the application of gallamine (10 μM) decreased the amplitude and duration of slow IPSPs, and therefore the rebound burst activity was not observed (Fig. 2*A*). To quantitatively examine the effect of gallamine on the IPSP, we applied repetitive electrical stimulations (30 s intervals) under the voltage clamp condition (holding potential, −60 mV) and observed changes in slow inhibitory postsynaptic currents (IPSCs) (Fig. 2*B* and *C*). We found that the prior bath application of gallamine reversibly attenuated the slow IPSCs (Fig. 2*B* and *C*), and this effect was significantly greater ($76.8 \pm 0.7\%$, calculated by dividing the averaged IPSC amplitude of 2.5–5.0 min after by that of 0 − 2.5 min before treatment; $n = 3$) than the vehicle applications ($6.0 \pm 4.7\%$, $P < 0.001$, $n = 4$; Fig. 2*G*). Application of another mAchR antagonist, scopolamine (20 μM), also abolished the slow IPSPs completely, and the firing activities of TN-GnRH neurones were little affected by electrical stimulation (Fig. 2*D*). This effect was further confirmed by voltage clamp experiments (1 μM scopolamine, Fig. 2*E* and *F*). Although we could not observe any recovery after washout (Fig. 2*F*), the prior bath application of scopolamine significantly decreased the amplitude of averaged IPSCs ($97.7 \pm 1.48\%$, $n = 3$) compared with the vehicle ($P < 0.001$; Fig. 2*G*) in this experiment.

Furthermore, we also performed a puffer application of Ach to the TN-GnRH neurones. We found that a puffer application of Ach resulted in immediate and strong hyperpolarisation of TN-GnRH neurones (Fig. 2*H*), as observed by the stimulation of fibres around

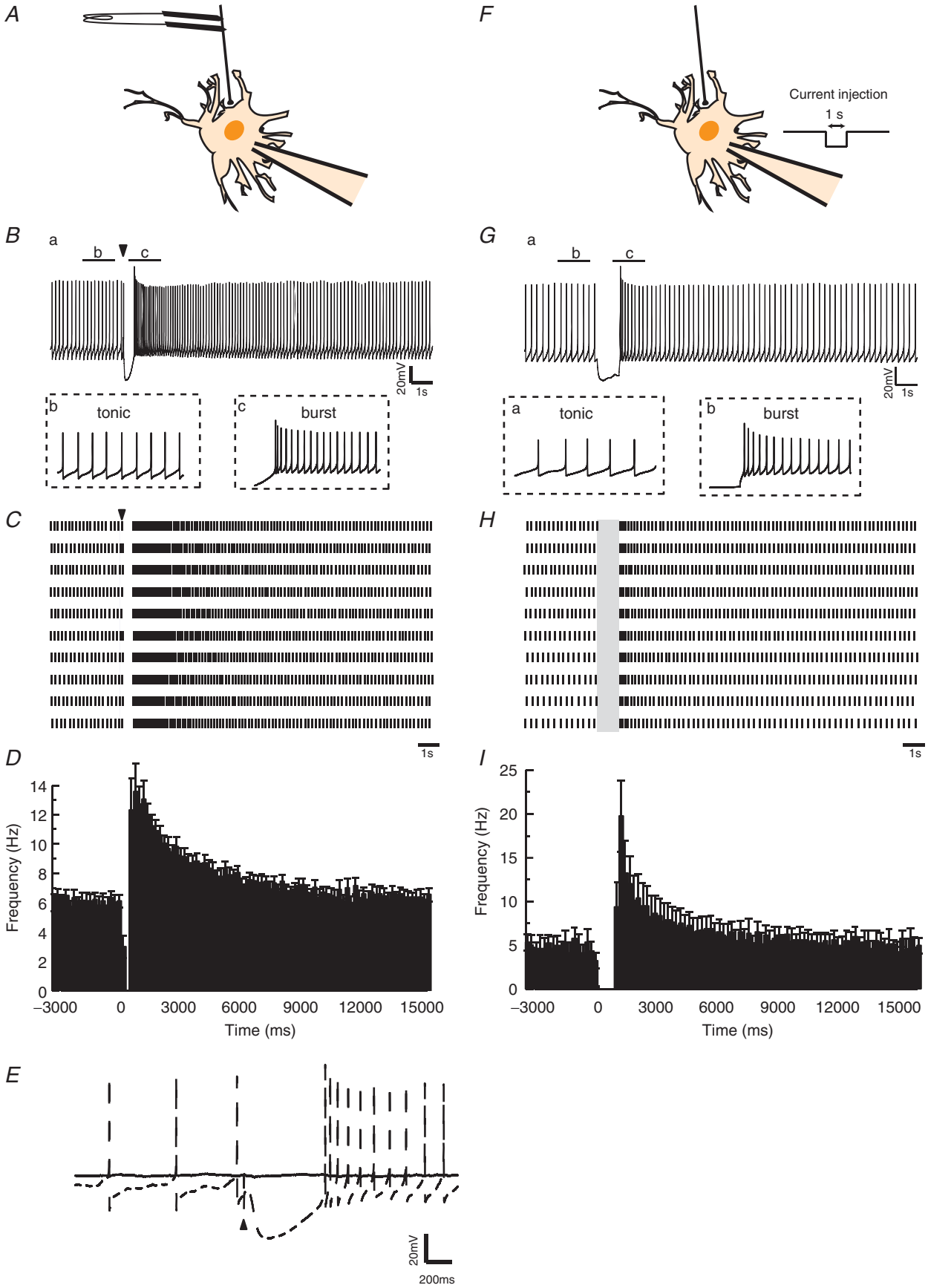

the TN-GnRH neurones. Taken together, these results strongly suggest that Ach is probably released from the axon terminals surrounding the cluster of TN-GnRH neurones, and the slow IPSP is induced by an activation of mAchR on the TN-GnRH neurones.

Cholinergic terminals surround proximal dendrites of TN-GnRH neurones

To confirm the morphological basis of cholinergic fibre innervations to the TN-GnRH neurones, we performed immunohistochemistry against a cholinergic neuronal marker, ChAT. Prominent ChAT-immunopositive fibres and terminal-like structures were labelled (Fig. 3*A*). These ChAT-positive terminals were abundantly distributed around the cluster of TN-GnRH neurones (Fig. 3*B* and *C*). Higher magnification photographs of these images clearly demonstrated that ChAT-immunoreactive terminal button-like structures (Fig. 3*D*) densely surround the proximal dendrites of TN-GnRH neurones (Fig. 3*E* and *F*). These results suggest that extrinsic cholinergic inputs of unknown origin give strong hyperpolarising drives that induce rebound burst activity of TN-GnRH neurones.

Potassium currents induced by mAchR activation

Then, we examined the ionic mechanisms underlying the slow IPSPs induced by the activation of mAchR. First, we measured the reversal potentials for the slow IPSC evoked by electrical stimulation in the voltage clamp mode in normal Ringer solution ($[K^+]_o = 3$ mM) and determined the reversal potential for the slow IPSC (-95.6 ± 7.98 mV; $n = 6$; Fig. 4*A* and *B*, left panel). Next, we changed the extracellular potassium concentrations and observed changes in the reversal potentials (-81.4 ± 7.53 mV ($n = 8$) in 6 mM $[K^+]_o$ and -64.8 ± 3.24 mV ($n = 4$) in 9 mM $[K^+]_o$; Fig. 4*A* and *B*, middle and right panels); these values were close to the values of the calculated equilibrium potentials for potassium ions (-75.5 mV and -65.2 mV in 6 and 9 mM $[K^+]_o$, respectively; Fig. 4*C*).

We also examined the reversal potentials for the slow IPSC by puffer application of Ach to TN-GnRH neurones. The reversal potentials for the Ach-induced currents are about -93.3 ± 1.12 mV, which is very similar to that of stimulation-induced slow IPSCs ($n = 6$; Fig. 4*D* and *E*). In addition, we found that the application of 500 μM Ba^{2+}, a less selective potassium channel blocker, reversibly diminished the Ach-induced currents (Fig. 5, decreased by 72.1 ± 3.3% of the value before treatment, calculated by dividing the averaged IPSC value of 2.5–5.0 min after by that of 0 − 2.5 min before Ba^{2+} treatment; $n = 4$). These results clearly demonstrate that mAchR activation opens potassium channels and hyperpolarises TN-GnRH neurones. We also examined the effect of 100 nM tertiapin-Q, a G protein-coupled inwardly rectifying potassium (GIRK) channel blocker, on the slow IPSCs to check whether mAchR is coupled to these channels. However, 100 nM tertiapin-Q did not show any prominent effects on slow IPSCs (Fig. S2, only decreased by 7.3 ± 5.7% of the value before treatment, calculated by dividing the averaged IPSC value of 2.5–4.0 min after by that of 0 − 1.5 min before tertiapin-Q treatment; $n = 3$).

Mechanism underlying the sustained rebound depolarisation after long hyperpolarisation

Finally, we attempted to identify the ionic mechanism that contributes to the generation of rebound burst

Figure 1. Current clamp recordings show that the tonic firing activities of terminal nerve (TN)-gonadotrophin releasing hormone (GnRH) neurones are switched to burst activities by a stimulation of fibres around them (*A–E*) or by a hyperpolarising current injection (*F–I*)
A, schematic drawing of the fibre stimulation. The firing activities of the TN-GnRH neurones were recorded by whole cell recording, and the fibres around the TN-GnRH neurone cell bodies were stimulated by a bipolar electrode. *B*, slow inhibitory postsynaptic potential (IPSP) was elicited by a single pulse stimulation of fibres surrounding the TN-GnRH neurones. A transient change from tonic firing to burst firing was also observed. The arrowhead indicates the time of the stimulus. *C*, raster plot showing that the activity of a TN-GnRH neurone is altered by the stimulation. Results of 10 repetitive trials from the same neurone are shown. The arrowhead indicates the time of stimulation. Scale bar, 1 s. *D*, averaged peristimulus time histogram (PSTH) showing the activities of TN-GnRH neurones ($n = 9$). The stimulation is applied at 0 ms. The time bin is 200 ms. *E*, application of tetrodotoxin (TTX) abolished the slow IPSP as well as the action potentials in the TN-GnRH neurone (the dashed and continuous line represent the traces before and during 0.75 μM TTX application, respectively). The arrowhead indicates stimulus artefact. Scale bar, 20 mV and 200 ms, respectively. *F*, schematic drawing of the experimental condition for injecting hyperpolarising current pulses to the TN-GnRH neurone. A whole cell patch-clamp electrode was used to record TN-GnRH neuronal activity and to apply hyperpolarising current pulses (1 s). The current amplitude was adjusted to the value that hyperpolarised the neurone by more than 20 mV. *G*, hyperpolarising current injection also induced a transient change in the firing frequency of the TN-GnRH neurones. *H*, raster plots showing that the activity of a TN-GnRH neurone is altered by the current injection. The grey box indicates the period of current injection. Results of 10 repetitive trials from the same neurone are shown. *I*, averaged PSTH showing the activities of TN-GnRH neurones. A hyperpolarising current is applied from 0 ms to 1000 ms. The time bin is 200 ms.

activities in TN-GnRH neurones. First, we perfused 0.75 μM TTX to the bath and found that large sustained rebound depolarisation remains after the injection of hyperpolarising current (Fig. 6*Aa*). This depolarising component after the hyperpolarisation appears to contribute to the rebound burst activities, and the rebound discharges are considered to be overlaid on these sustained depolarisations in TN-GnRH neurones. To identify the

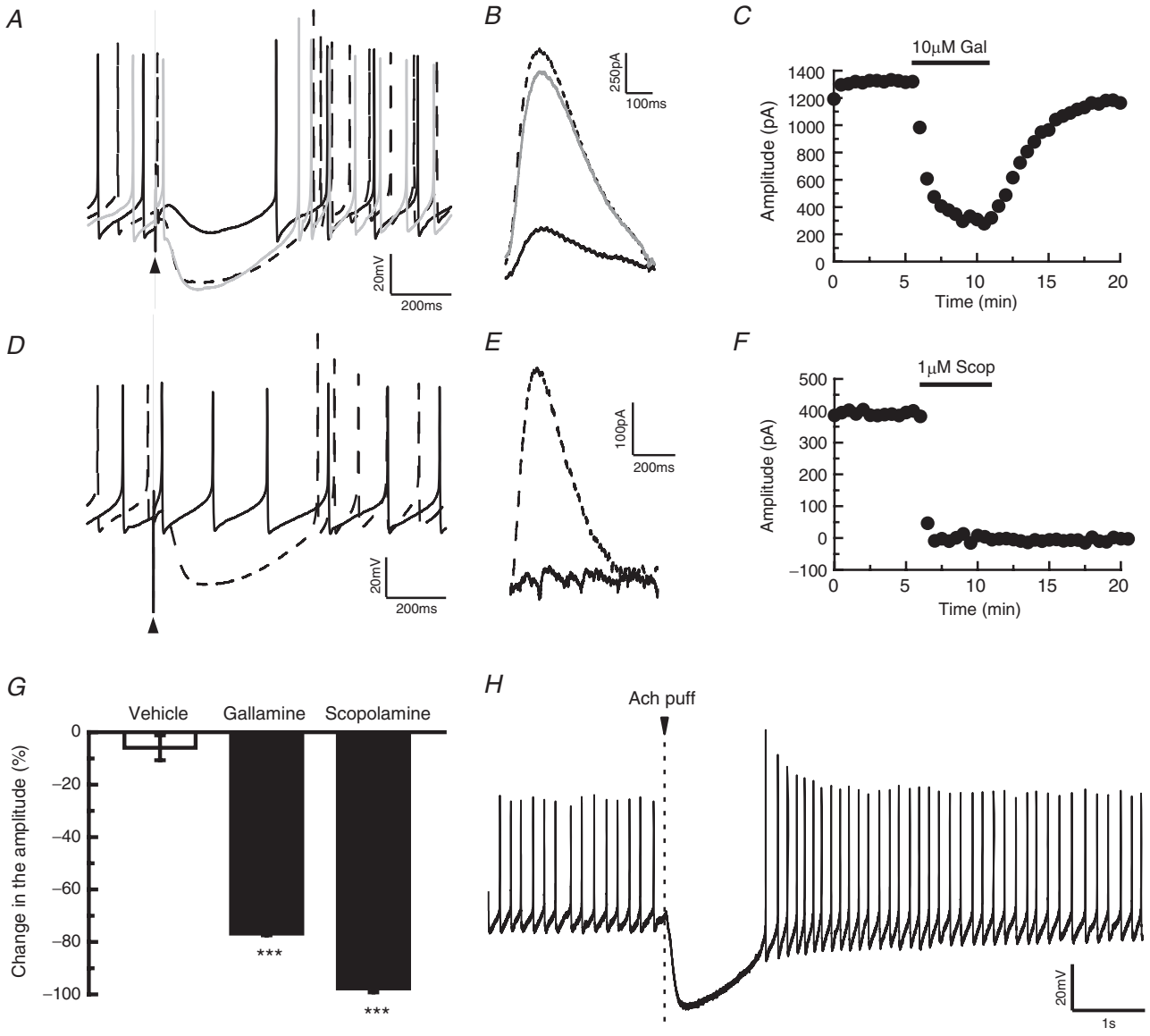

Figure 2. The slow inhibitory postsynaptic potential (IPSP) is induced by the activation of muscarinic acetylcholine (Ach) receptors

A, *B*, attenuation of slow IPSP (current clamp; *A*) or inhibitory postsynaptic current (IPSC) (voltage clamp; *B*) by the application of gallamine (10 μM). The dashed black line, solid black line and grey line represent traces before, during and after gallamine applications. *C*, time course of the effect of gallamine (10 μM) on the amplitude of slow IPSC. *D*, *E*, current clamp recordings (*D*) or voltage clamp recordings (*E*) showing that the application of scopolamine abolished slow IPSP or IPSC (dashed line and continuous line represent traces before and during scopolamine applications, 20 μM and 1 μM in *D* and *E*, respectively). *F*, time course of the effect of scopolamine (1 μM) on the amplitude of slow IPSC. *G*, statistical comparison of the gallamine-induced ($n = 3$) and scopolamine-induced ($n = 3$) suppression of slow IPSC of the terminal nerve (TN)-gonadotrophin releasing hormone (GnRH) neurones in comparison with the vehicle application ($n = 4$). The averaged amplitude of 0.0–2.0 min before treatment was normalised to 100% and the averaged amplitude of 2.5–5.0 min after treatment was compared with this value. ***$P < 0.001$, Dunnett's test. *H*, puffer application of Ach (1 mM) on the TN-GnRH neurone immediately evoked a strong hyperpolarisation of the TN-GnRH neurone. Arrowhead indicates the time of Ach puffer application.

major current component(s) that form the sustained rebound depolarisation, we examined the effects of several pharmacological agents in the presence of TTX. Because we found that extracellular Na^+ substitution changed the resting membrane potentials of TN-GnRH neurones (see also Oka, 1995) and therefore should affect the waveform of the rebound depolarisation (Fig. S3), we kept the membrane potentials to the value before treatment (ranging from −40 to −50 mV) by injecting constant DC current to the recorded neurones during the Na^+

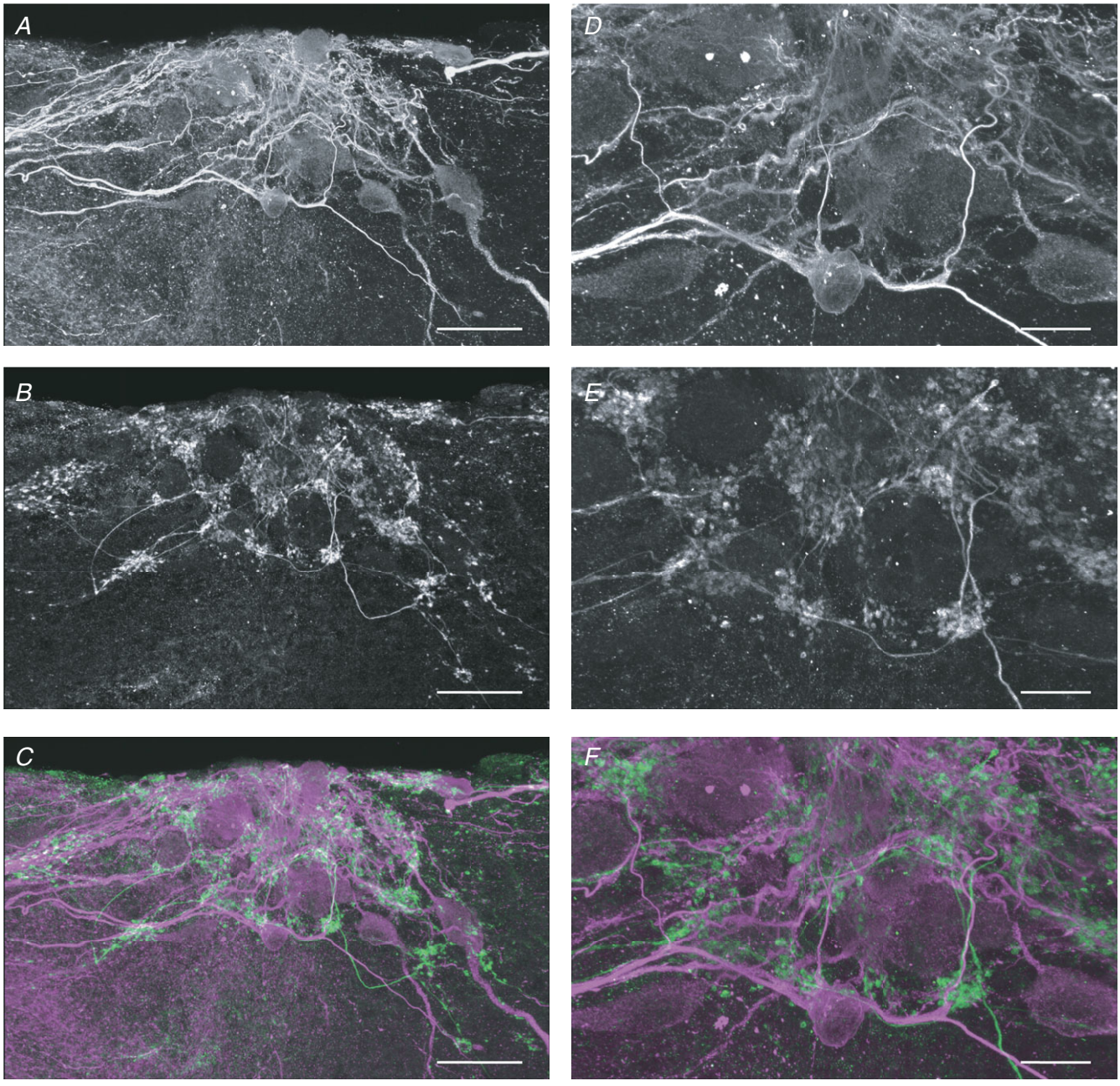

Figure 3. Confocal microscopy images of a cell cluster of terminal nerve (TN)-gonadotrophin releasing hormone (GnRH) neurones double-labelled with anti-choline acetyltransferase (anti-ChAT) antiserum and anti-microtubule-associated protein (MAP)2a + 2b monoclonal antibody
A, immunoreactive fluorescent signals against MAP2a + 2b show the location of the somata and dendrites of TN-GnRH neurones in the cell cluster of goldfish olfactory bulb. *B*, fluorescent signals against ChAT antiserum show the location of cholinergic neuroterminals around the TN-GnRH neurones. *C*, merged image of MAP2a + 2b (magenta) and ChAT (green) immunocytochemistry. *D–F*, higher magnification images of the central regions of *A–C*. Dense distribution of ChAT-immunoreactive terminal buttons was observed around the dendrite and soma of TN-GnRH neurones. Scale bar: 50 μm (*A–C*); 20 μm (*D–F*).

substitution experiments. The value of the liquid junction potential between the standard external solution and the Na^+-substituted solution (4.7 mV) was considered in the experiment, and was also corrected off-line.

We found that a combination of extracellular substitution of Na^+ with NMDG and application of Ni^{2+} [1 mM; a broad-spectrum blocker of voltage-gated calcium channels (VGCCs)] greatly attenuated both the amplitude and averaged value (first 5 s) of rebound depolarisations ($n = 7$, decreased by $61.4 \pm 16.7\%$ and $69.0 \pm 13.0\%$ in amplitude and averaged value, respectively; Fig. 6*Ad* and *B*; $P < 0.05$ in both) in TN-GnRH neurones. We also tried a combination of extracellular substitution of Na^+ with NMDG and a lower concentration of Ni^{2+} (200 μM; predominantly blocking low-voltage-activated (LVA or T-type) Ca^{2+} channels) in order to characterise the subtype of VGCCs that are involved in the generation of rebound depolarisations. We found that its suppressive

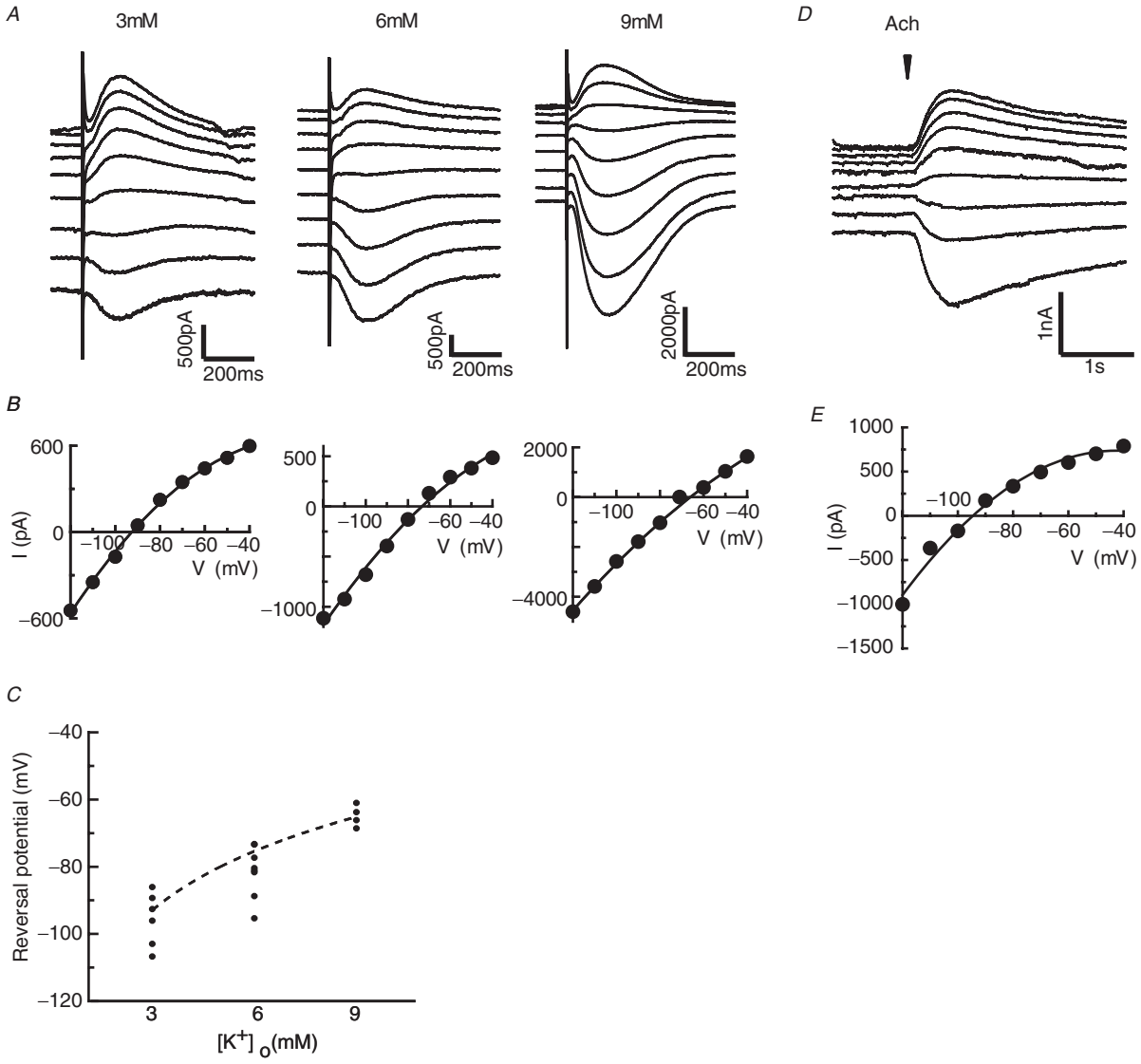

Figure 4. Reversal potential values of the slow inhibitory postsynaptic current (IPSC) are consistent with the values for the calculated equilibrium potentials for potassium ions
A, slow IPSCs recorded at different holding potentials ranging from –120 to −40 mV (10 mV step) in 3, 6 and 9 mM $[K^+]_o$. *B*, *I–V* plot of the peak value of slow IPSCs obtained from the current responses. *C*, average value of reversal potentials is consistent with the calculated equilibrium potentials for potassium ions in 3, 6 and 9 mM $[K^+]_o$. Each small dot indicates each data point, and the dashed line denotes the equilibrium potentials of potassium ions calculated from the Nernst equation. *D*, acetylcholine (Ach)-induced currents recorded at different holding potentials ranging from −120 to −40 mV. The reversal potential of slow IPSC evoked by puffer application of Ach is consistent with that by electrical stimulation of the surrounding fibres. The arrowhead indicates the time of Ach puffer application. *E*, *I–V* plot of the peak value of Ach-induced currents obtained from the traces shown in (*D*).

effect on the rebound depolarisations was comparable with that of 1 mM Ni^{2+} in Na^+-free solution ($n = 5$, decreased by 60.9 ± 19.0% and 74.6 ± 9.9% in amplitude and averaged value, respectively; Fig. 6*Ae* and *B*; $P = 0.064$ and $P < 0.05$, respectively). Such an attenuation of the rebound depolarisation was not observed during the application of 1 mM Ni^{2+} alone (Fig. 6*Ab*). Substitution of extracellular Na^+ with NMDG alone did not diminish the rebound depolarisations, but slightly modified the waveform; it significantly delayed the onset and slightly increased the amplitude of the rebound depolarisations (Fig. 6*Ac* and *Bc*).

Discussion

Rebound burst activities in TN-GnRH neurones

In this study, we found that a single pulse stimulation of the surrounding fibres reproducibly induced rebound burst activities in TN-GnRH neurones. This rebound burst activity occurred following a slow IPSP that was mediated by the activation of mAchRs in TN-GnRH neurones. Activation of the mAchRs induced the opening of potassium channels and evoked strong hyperpolarisation in TN-GnRH neurones, and this hyperpolarisation was followed by rebound burst activity.

The phenomenon of rebound burst activity has already been reported in the deep cerebellar nuclear neurones (Aizenman & Linden, 1999). It was reported that a high-frequency train of IPSPs evoked a rebound burst or increases in spike numbers in these neurones (Aizenman & Linden, 1999; Tadayonnejad *et al.* 2010). In this study, the firing frequency of TN-GnRH neurones (5.97 ± 1.32 Hz; $n = 9$) was increased to 37.5 ± 8.90 Hz (maximum) by a single stimulus to the fibres surrounding them. Previous studies have suggested that high-frequency firings, possibly more than about 10 Hz, are important for the release of neuropeptides (Dutton & Dyball, 1979; Ishizaki *et al.* 2004; Liu *et al.* 2011). Considering these reports, it is highly possible that the rebound burst activities observed in TN-GnRH neurones can potentially function to elicit the release of GnRH and other peptides, such as neuropeptide FF, which are produced by these neurones (see Saito *et al.* 2010).

Slow IPSPs mediated by cholinergic inputs

In this study, we observed that a single pulse stimulation to fibres surrounding TN-GnRH neurones induced a slow IPSP. Similar slow IPSP-like potential change has been reported previously in the carp TN-GnRH neurones (Fujita *et al.* 1985), although the authors did not mention the occurrence of rebound burst activities or candidate neurotransmitters or the ionic mechanisms underlying them. In our study, slow IPSPs of TN-GnRH neurones were considered to be mediated by Ach, because they were blocked by the application of the antagonist of mAchRs. Furthermore, the activation of mAchRs has been suggested to hyperpolarise TN-GnRH neurones by opening potassium channels. A similar mechanism of slow IPSP has been reported in the rat striatal cholinergic

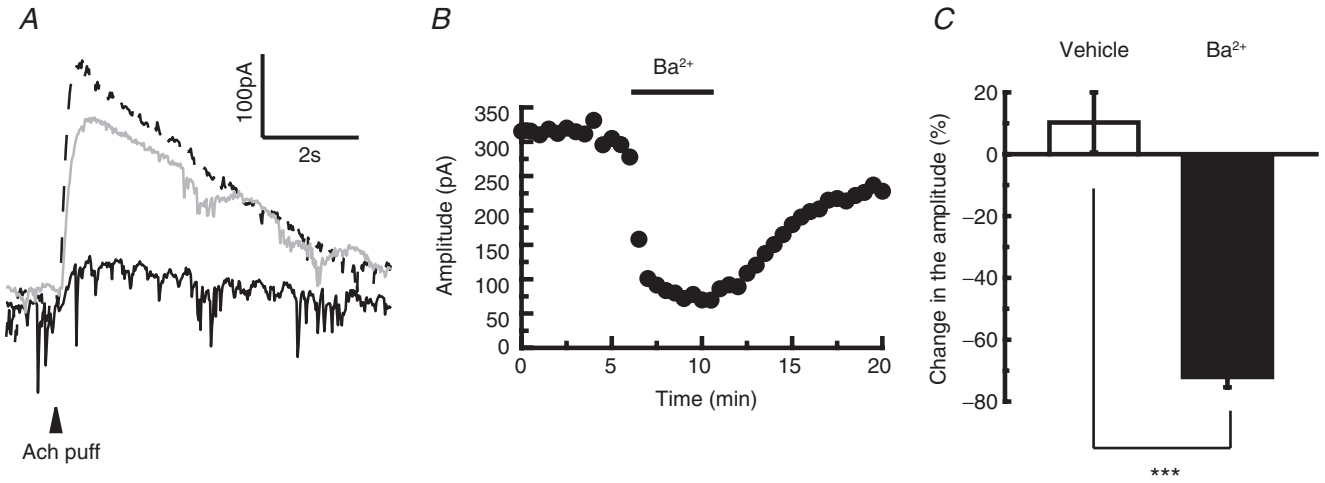

Figure 5. Prior bath application of Ba^{2+} reversibly diminishes acetylcholine (Ach)-induced outward currents in the terminal nerve (TN)-gonadotrophin releasing hormone (GnRH) neurones
A, representative traces showing the effect of Ba^{2+} on the Ach-induced currents (dashed line, continuous line and grey line represent traces before, during and after 500 μM Ba^{2+} application, respectively). The arrowhead indicates the time of Ach puffer application. *B*, time course of the effect of 500 μM Ba^{2+} application on the amplitude of Ach-induced currents. *C*, statistical comparison of the effect of Ba^{2+} on Ach-induced currents ($n = 4$) in comparison with the vehicle application ($n = 5$). The averaged amplitude of 3.0–5.5 min in (*B*) was normalised to 100% and the averaged value of 8.0–10.5 min was compared with the former. ***$P < 0.001$.

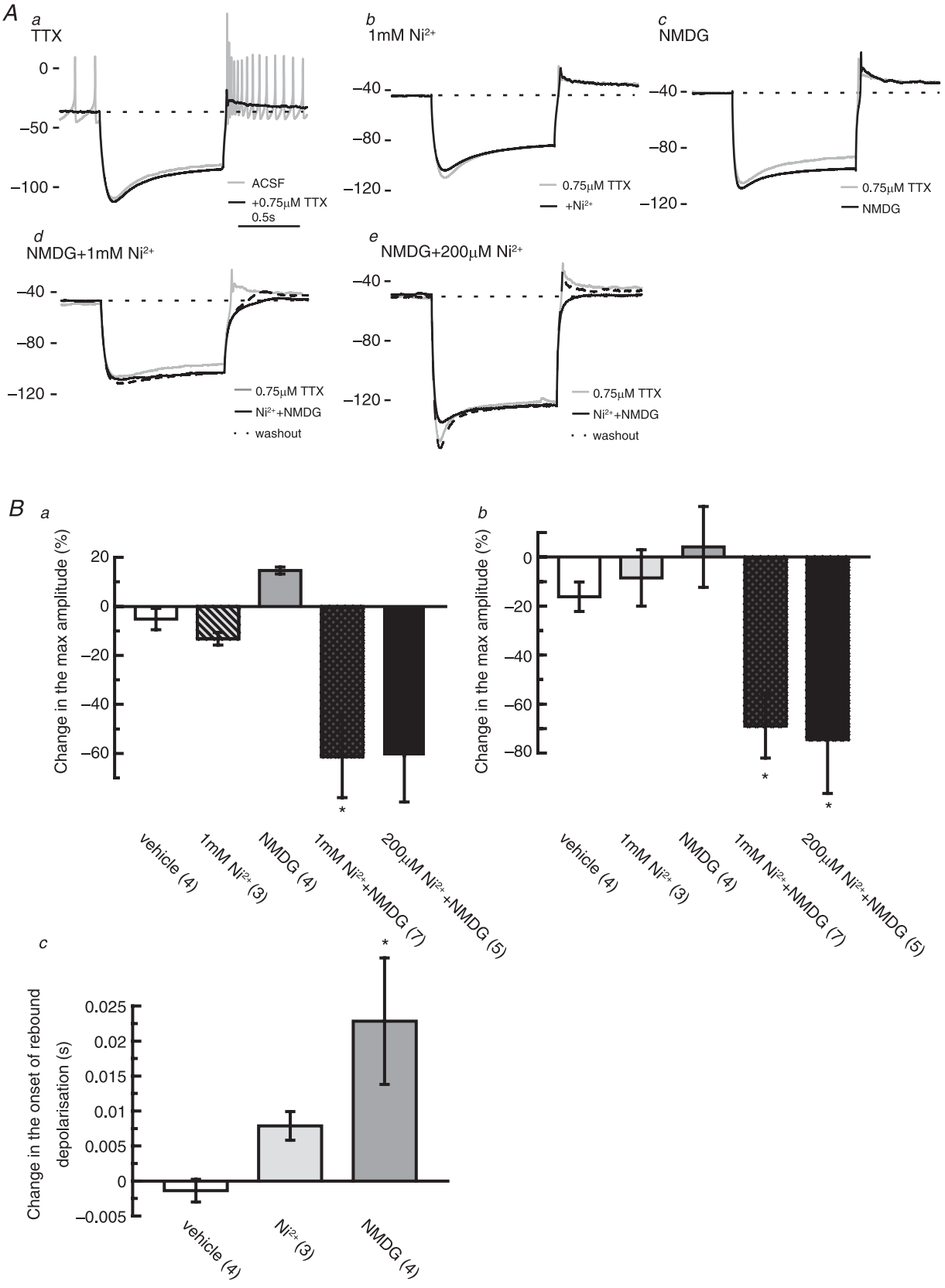

interneurones (Calabresi *et al.* 1998). Here, a single pulse stimulation of the rat striatum slice elicited a hyperpolarising IPSP in the striatal cholinergic interneurones, indicating the existence of an auto-inhibitory mechanism among the striatal cholinergic neurones. This IPSP lasted for 0.5–1.0 s, and was also mediated by the activation of mAchRs and the opening of potassium channels. It is noteworthy that there are some reports suggesting that the activation of mAchRs evokes the opening of potassium channels and elicits hyperpolarisations of these neurones, although the detailed mechanisms, such as the molecular identities of the potassium channel subtypes and the intracellular signal transduction mechanisms underlying these phenomena, have not been identified (Pan & Williams, 1994; Yang *et al.* 2010). Our result that tertiapin-Q did not block the slow IPSCs suggests that GIRK channels are not involved in this process. A similar result has also been reported in cholinergic action on suprachiasmatic nucleus neurones (Yang *et al.* 2010). Possibly, there may be a general signal transduction cascade for the opening of potassium channels by the activation of mAchR in many neurones.

Origins of cholinergic inputs to TN-GnRH neurones

In this study, slow IPSPs could be observed by a single pulse, not a high-frequency train, of stimulation to the fibres around TN-GnRH neurones. Thus, the firing activity of TN-GnRH neurones appears to be strongly regulated by the cholinergic fibres surrounding them. Our anatomical analysis revealed that the cell bodies of TN-GnRH neurones were densely surrounded by ChAT-immunoreactive button-like terminals. Although it has been reported that ChAT-immunoreactive neurones exist in the TN of zebrafish and bonnethead shark (Edwards *et al.* 2007; Moeller & Meredith, 2010), we did not observe any ChAT-immunoreactive cell bodies in TN, even when we used the same kind of antibodies as employed in these previous studies (data not shown).

The existence of the cholinergic button-like structures in this study supports the electrophysiological data showing that only a single pulse stimulus of cholinergic fibres efficiently evokes strong hyperpolarisation in TN-GnRH neurones. Here, it may be important to discuss the origins of cholinergic inputs that densely surround TN-GnRH neurones. In mammals, it has been shown that cholinergic neurones located at the basal forebrain innervate the olfactory bulb (Ichikawa & Hirata, 1986), regulating the information processing of the olfactory bulbar neural circuits (Tsuno *et al.* 2008). Because TN-GnRH neurones are located in the rostral area of the olfactory bulb in goldfish, these cholinergic fibres may project to the TN as well as the olfactory bulb. Importantly, these cholinergic neurones in the basal forebrain show behavioural state-dependent changes in their activities (Manns *et al.* 2000). Thus, the neuromodulatory action of these cholinergic neurones on the olfactory bulb is dependent on the arousal state of the animal (Tsuno *et al.* 2008). In this context, it is possible that this cholinergic system promotes the release of GnRH from TN-GnRH neurones, dependent on the arousal state. Importantly, the TN-GnRH system has been suggested to affect the motivational or arousal state of the animal (Yamamoto *et al.* 1997; Kawai *et al.* 2009). For example, lesion of the TN resulted in a decrease in motivation for reproductive behaviour in male hamsters (Wirsig & Leonard, 1987) or dwarf gourami, a model animal for studies of the TN (Yamamoto *et al.* 1997). It may be suggested that TN-GnRH neurones partially mediate the cholinergic action, which results in behavioural arousal in animals.

Ionic mechanism underlying rebound depolarisations

In this study, we demonstrated that a slow IPSP resulted in rebound burst activity of TN-GnRH neurones. Here, the ionic mechanisms underlying the rebound depolarisations are also of interest. In this study,

Figure 6. The slow rebound depolarisation consists of the combinational components of tetrodotoxin (TTX)-resistant persistent voltage-gated Na^+ channels and low-voltage-activated Ca^{2+} channels
A, representative traces showing the effects of each pharmacological manipulation on the rebound depolarisations in the terminal nerve (TN)-gonadotrophin releasing hormone (GnRH) neurones. *Aa*, an application of TTX revealed that sustained rebound depolarisation follows the offset of the hyperpolarisation of the TN-GnRH neurone (grey, before 0.75 μM TTX application; black, during 0.75 μM TTX application). Dashed line denotes the baseline membrane potential before the current injection. Bath application of 1 mM Ni^{2+} (*Ab*) and substitution of extracellular Na^+ with *N*-methyl-D-glucamine (NMDG) (*Ac*) did not diminish the rebound depolarisations in the presence of 0.75 μM TTX. Alternatively, sustained rebound depolarisation was diminished by bath application of 1 mM Ni^{2+} in Na^+-free solution (*Ad*) or 200 μM Ni^{2+} in Na^+-free solution (*Ae*) in the presence of 0.75 μM TTX (grey line, solid black line and dashed black line represent before, during and after Ni^{2+} + NMDG, respectively). The values on the left of the traces denote the membrane potentials. Scale bar, 1 s. *B*, Statistical comparisons of the effects of pharmacological manipulations on the rebound depolarisation. The response 0.5 min before treatment was normalised to 100%, and the value 4 min after treatment was examined. *Ba*, normalised change in the amplitudes of the rebound depolarisations. *Bb*, normalised change in the averaged value (first 5 s) of the rebound depolarisations. *Bc*, change in the onset of rebound depolarisations. Numbers in parentheses represent the numbers of neurones tested for the experiment. $^*P < 0.05$, Dunnett's test.

we revealed that the slow IPSP evokes rebound burst activities in TN-GnRH neurones. A similar phenomenon was observed by hyperpolarising current injections in TN-GnRH neurones, suggesting that voltage-dependent conductance is important for the rebound burst activity. Here, we discuss its possible mechanisms. In TN-GnRH neurones, TTX-resistant persistent Na^+ current drives the depolarisation at subthreshold membrane potential, contributing to the generation of pacemaker activity. The steady-state inactivation curve of the TTX-resistant persistent voltage-gated sodium channels (VGSCs) is in the range of about −100 to 0 mV in TN-GnRH neurones, whereas their activation curve is in the range of about −60 to 0 mV, thus showing the wide range of window currents near the resting membrane potentials (Oka, 1996). Furthermore, TN-GnRH neurones show LVA Ca^{2+} currents. The steady-state inactivation of LVA Ca^{2+} currents greatly increases between −80 and −40 mV, whereas its activation begins at −80 mV (Haneda & Oka, 2004). From these results, it is highly possible that the hyperpolarisation induced by Ach relieves the inactivation of the persistent VGSCs and/or VGCCs (LVA Ca^{2+} currents) and shows sustained rebound depolarisation in TN-GnRH neurones. Alternatively, ion influx other than VGSC or VGCC may also be involved in the rebound depolarisation. For example, non-selective cation channels, such as the transient receptor potential channel, which is expressed in TN-GnRH neurones (Umatani *et al.* 2013), or the hyperpolarisation-activated cation channel, could contribute.

In this study, simultaneous blockade of Na^+ and Ca^{2+} influx could attenuate the rebound depolarisation of TN-GnRH neurones, but single blockades of Na^+ or Ca^{2+} alone could not. Furthermore, we found that the suppressive effect of a low concentration of Ni^{2+} in Na^+-free solution on rebound depolarisations is comparable with that of 1 mM Ni^{2+} in Na^+-free solution, suggesting that the LVA Ca^{2+} current is mainly involved in the generation of rebound depolarisation. These results suggest that persistent VGSCs and LVA Ca^{2+} current can contribute to the rebound depolarisations in TN-GnRH neurones, and there may be compensatory mechanisms consisting of these channels (summarised in Fig. 7). Importantly, the conductance of persistent VGSCs and LVA Ca^{2+} current has also been reported in other neurosecretory cells, such as vasopressin and hypothalamic GnRH neurones (Fisher & Bourque, 1995; Sabatier *et al.* 1997; Tanaka *et al.* 1999; Kato *et al.* 2009; Zhang *et al.* 2009; Wang *et al.* 2010). Thus, a similar mechanism may also work in these neurones for the release of their neuropeptides.

It should also be noted that substitution of extracellular Na^+ with NMDG slightly modified the waveform of rebound depolarisation (delayed onset and slightly increased amplitude) compared with vehicle or Ni^{2+} application. Although it is difficult to confirm the underlying mechanisms, there are several possibilities to explain this. First, removal of extracellular Na^+ can affect various intracellular compositions that are normally balanced by the transporters, such as Na^+/Ca^{2+} exchange (Grierson *et al.* 1992). Possibly, the increase in intracellular Ca^{2+} may modulate the characteristics of ion channels that are involved in the rebound depolarisation in the present experiment, thus altering its waveform. Second, the removal of extracellular Na^+ can reduce the conductance of hyperpolarisation-activated cation channels (Chen, 1997), thus showing stronger hyperpolarisation during hyperpolarising current injection. This strong hyperpolarisation may more efficiently relieve the inactivation of voltage-gated channels that are involved in the generation of rebound depolarisation. As a result, the amplitude of the rebound depolarisation could be increased.

Overall, the present findings implicate a novel cholinergic pathway that regulates the burst activities of TN-GnRH neurones. We found that cholinergic neurones are strong regulators of TN-GnRH neurones. Future studies concerning the relationship between the activity of these cholinergic neurones and TN-GnRH neurones should help us to understand the unresolved interactive mechanisms between these distinct neuromodulatory systems.

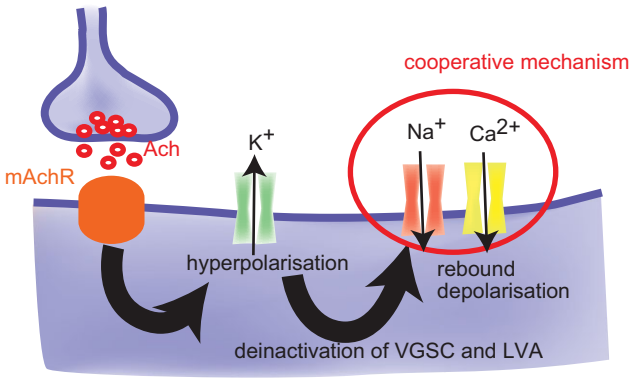

Figure 7. A proposed mechanism underlying the slow inhibitory postsynaptic potential (IPSP) and the rebound burst activities in terminal nerve (TN)-gonadotrophin releasing hormone (GnRH) neurones
Stimulation of the cholinergic fibres around the TN-GnRH neurones activates the muscarinic acetylcholine receptors (mAchR) on the TN-GnRH neurones. This results in the opening of potassium channels, showing a large and long hyperpolarisation of TN-GnRH neurones. The long hyperpolarisation relieves the inactivation of persistent voltage-gated Na^+ channels (VGSCs) and low-voltage-activated (LVA) Ca^{2+} channels. Cooperative action of persistent VGSCs and LVA Ca^{2+} channels generates the rebound depolarisations, which evoke the rebound burst discharges in the TN-GnRH neurones.

References

Abe H & Oka Y (1999). Characterization of K^+ currents underlying pacemaker potentials of fish gonadotropin-releasing hormone cells. *J Neurophysiol* **81**, 643–653.

Abramoff MD, Magalhaes PJ & Ram SJ (2004). Image processing with ImageJ. *Biophoton Int* **11**, 36–42.

Aizenman CD & Linden DJ (1999). Regulation of the rebound depolarization and spontaneous firing patterns of deep nuclear neurons in slices of rat cerebellum. *J Neurophysiol* **82**, 1697–1709.

Calabresi P, Centonze D, Pisani A, Sancesario G, North RA & Bernardi G (1998). Muscarinic IPSPs in rat striatal cholinergic interneurones. *J Physiol* **510**, 421–427.

Castel M, Morris J & Belenky M (1996). Non-synaptic and dendritic exocytosis from dense-cored vesicles in the suprachiasmatic nucleus. *Neuroreport* **7**, 543–547.

Chen C (1997). Hyperpolarization-activated current (Ih) in primary auditory neurons. *Hear Res* **110**, 179–190.

Drummond GB (2009). Reporting ethical matters in the Journal of Physiology: standards and advice. *J Physiol* **587**, 713–719.

Dutton A & Dyball RE (1979). Phasic firing enhances vasopressin release from the rat neurohypophysis. *J Physiol* **290**, 433–440.

Edwards JG, Greig A, Sakata Y, Elkin D & Michel WC (2007). Cholinergic innervation of the zebrafish olfactory bulb. *J Comp Neurol* **504**, 631–645.

Eisthen HL, Delay RJ, Wirsig-Wiechmann CR & Dionne VE (2000). Neuromodulatory effects of gonadotropin releasing hormone on olfactory receptor neurons. *J Neurosci* **20**, 3947–3955.

Fisher TE & Bourque CW (1995). Voltage-gated calcium currents in the magnocellular neurosecretory cells of the rat supraoptic nucleus. *J Physiol* **486**, 571–580.

Fujita I, Satou M & Ueda K (1985). Ganglion cells of the terminal nerve: morphology and electrophysiology. *Brain Res* **335**, 148–152.

Grierson JP, Petroski RE, O'Connell SM & Geller HM (1992). Calcium homeostasis in dissociated embryonic neurons: a flow cytometric analysis. *J Neurophysiol* **67**, 704–714.

Haneda K & Oka Y (2004). Selective modulation of voltage-gated calcium channels in the terminal nerve gonadotropin-releasing hormone neurons of a teleost, the dwarf gourami (Colisa lalia). *Endocrinology* **145**, 4489–4499.

Haneda K & Oka Y (2008). Coordinated synchronization in the electrically coupled network of terminal nerve gonadotropin-releasing hormone neurons as demonstrated by double patch-clamp study. *Endocrinology* **149**, 3540–3548.

Ichikawa T & Hirata Y (1986). Organization of choline acetyltransferase-containing structures in the forebrain of the rat. *J Neurosci* **6**, 281–292.

Ishizaki M, Iigo M, Yamamoto N & Oka Y (2004). Different modes of gonadotropin-releasing hormone (GnRH) release from multiple GnRH systems as revealed by radioimmunoassay using brain slices of a teleost, the dwarf gourami (*Colisa lalia*). *Endocrinology* **145**, 2092–2103.

Johnson CD & Epstein ML (1986). Monoclonal antibodies and polyvalent antiserum to chicken choline acetyltransferase. *J Neurochem* **46**, 968–976.

Jan YN & Jan LY (1983). A LHRH-like peptidergic neurotransmitter capable of "action at a distance" in autonomic ganglia. *Trends Neurosci* **6**, 320–325.

Kato M, Tanaka N, Ishii H, Yin C & Sakuma Y (2009). Ca^{2+} channels and Ca^{2+}-activated K^+ channels in adult rat gonadotrophin-releasing hormone neurones. *J Neuroendocrinol* **21**, 312–315.

Kawai T, Abe H, Akazome Y & Oka Y (2010). Neuromodulatory effect of GnRH on the synaptic transmission of the olfactory bulbar neural circuit in goldfish, *Carassius auratus*. *J Neurophysiol* **104**, 3540–3550.

Kawai T, Oka Y & Eisthen H (2009). The role of the terminal nerve and GnRH in olfactory system neuromodulation. *Zoolog Sci* **26**, 669–680.

Kim KH, Patel L, Tobet SA, King JC, Rubin BS & Stopa EG (1999). Gonadotropin-releasing hormone immunoreactivity in the adult and fetal human olfactory system. *Brain Res* **826**, 220–229.

Kim MH, Oka Y, Amano M, Kobayashi M, Okuzawa K, Hasegawa Y, Kawashima S, Suzuki Y & Aida K (1995). Immunocytochemical localization of sGnRH and cGnRH-II in the brain of goldfish, *Carassius auratus*. *J Comp Neurol* **356**, 72–82.

Kinoshita M, Kobayashi S, Urano A & Ito E (2007). Neuromodulatory effects of gonadotropin-releasing hormone on retinotectal synaptic transmission in the optic tectum of rainbow trout. *Eur J Neurosci* **25**, 480–484.

Leng G & Ludwig M (2006). Jacques Benoit Lecture. Information processing in the hypothalamus: peptides and analogue computation. *J Neuroendocrinol* **18**, 379–392.

Liu X, Porteous R, d'Anglemont de Tassigny X, Colledge WH, Millar R, Petersen SL & Herbison AE (2011). Frequency-dependent recruitment of fast amino acid and slow neuropeptide neurotransmitter release controls gonadotropin-releasing hormone neuron excitability. *J Neurosci* **31**, 2421–2430.

Ludwig M & Leng G (2006). Dendritic peptide release and peptide-dependent behaviours. *Nat Rev Neurosci* **7**, 126–136.

Manns ID, Alonso A & Jones BE (2000). Discharge properties of juxtacellularly labelled and immunohistochemically identified cholinergic basal forebrain neurons recorded in association with the electroencephalogram in anaesthetized rats. *J Neurosci* **20**, 1505–1518.

Maruska KP & Tricas TC (2011). Gonadotropin-releasing hormone (GnRH) modulates auditory processing in the fish brain. *Horm Behav* **59**, 451–464.

Moeller JF & Meredith M (2010). Differential co-localization with choline acetyltransferase in nervus terminalis suggests functional differences for GnRH isoforms in bonnethead sharks (*Sphyrna tiburo*). *Brain Res* **1366**, 44–53.

Oka Y (1995). Tetrodotoxin-resistant persistent Na^+ current underlying pacemaker potentials of fish gonadotrophin-releasing hormone neurones. *J Physiol* **482**, 1–6.

Oka Y (1996). Characterization of TTX-resistant persistent Na^+ current underlying pacemaker potentials of fish gonadotropin-releasing hormone (GnRH) neurons. *J Neurophysiol* **75**, 2397–2404.

Oka Y & Ichikawa M (1990). Gonadotropin-releasing hormone (GnRH) immunoreactive system in the brain of the dwarf gourami (*Colisa lalia*) as revealed by light microscopic immunocytochemistry using a monoclonal antibody to common amino acid sequence of GnRH. *J Comp Neurol* **300**, 511–522.

Oka Y & Ichikawa M (1991). Ultrastructure of the ganglion cells of the terminal nerve in the dwarf gourami (*Colisa lalia*). *J Comp Neurol* **304**, 161–171.

Oka Y & Ichikawa M (1992). Ultrastructural characterization of gonadotropin-releasing hormone (GnRH)-immunoreactive terminal nerve cells in the dwarf gourami. *Neurosci Lett* **140**, 200–202.

Oka Y & Matsushima T (1993). Gonadotropin-releasing hormone (GnRH)-immunoreactive terminal nerve cells have intrinsic rhythmicity and project widely in the brain. *J Neurosci* **13**, 2161–2176.

Pan ZZ & Williams JT (1994). Muscarine hyperpolarizes a subpopulation of neurons by activating an M2 muscarinic receptor in rat nucleus raphe magnus in vitro. *J Neurosci* **14**, 1332–1338.

Park D & Eisthen HL (2003). Gonadotropin releasing hormone (GnRH) modulates odorant responses in the peripheral olfactory system of axolotls. *J Neurophysiol* **90**, 731–738.

Sabatier N, Richard P & Dayanithi G (1997). L-, N- and T- but neither P- nor Q-type Ca^{2+} channels control vasopressin-induced Ca^{2+} influx in magnocellular vasopressin neurones isolated from the rat supraoptic nucleus. *J Physiol* **503**, 253–268.

Saito TH, Nakane R, Akazome Y, Abe H & Oka Y (2010). Electrophysiological analysis of the inhibitory effects of FMRFamide-like peptides on the pacemaker activity of gonadotropin-releasing hormone neurons. *J Neurophysiol* **104**, 3518–3529.

Salio C, Lossi L, Ferrini F & Merighi A (2006). Neuropeptides as synaptic transmitters. *Cell Tissue Res* **326**, 583–598.

Tadayonnejad R, Anderson D, Molineux ML, Mehaffey WH, Jayasuriya K & Turner RW (2010). Rebound discharge in deep cerebellar nuclear neurons in vitro. *Cerebellum* **9**, 352–374.

Tanaka M, Cummins TR, Ishikawa K, Black JA, Ibata Y & Waxman SG (1999). Molecular and functional remodeling of electrogenic membrane of hypothalamic neurons in response to changes in their input. *Proc Natl Acad Sci U S A* **96**, 1088–1093.

Tsuno Y, Kashiwadani H & Mori K (2008). Behavioral state regulation of dendrodendritic synaptic inhibition in the olfactory bulb. *J Neurosci* **28**, 9227–9238.

Umatani C, Abe H & Oka Y (2013). Neuropeptide RFRP inhibits the pacemaker activity of terminal nerve GnRH neurons. *J Neurophysiol* 109:2354–2363.

Wan Y, Otsuna H, Chien CB & Hansen C (2009). An interactive visualization tool for multi-channel confocal microscopy data in neurobiology research. *IEEE Trans Vis Comput Graph* **15**, 1489–1496.

Wang Y, Garro M & Kuehl-Kovarik MC (2010). Estradiol attenuates multiple tetrodotoxin-sensitive sodium currents in isolated gonadotropin-releasing hormone neurons. *Brain Res* **1345**, 137–145.

Wayne NL, Kuwahara K, Aida K, Nagahama Y & Okubo K (2005). Whole-cell electrophysiology of gonadotropin-releasing hormone neurons that express green fluorescent protein in the terminal nerve of transgenic medaka (*Oryzias latipes*). *Biol Reprod* **73**, 1228–1234.

Whitnall MH & Gainer H (1985). Ultrastructural immunolocalization of vasopressin and neurophysin in neurosecretory cells of dehydrated rats. *Brain Res* **361**, 400–404.

Wirsig CR & Leonard CM (1987). Terminal nerve damage impairs the mating behaviour of the male hamster. *Brain Res* **417**, 293–303.

Yamamoto N & Ito H (2000). Afferent sources to the ganglion of the terminal nerve in teleosts. *J Comp Neurol* **428**, 355–375.

Yamamoto N, Oka Y & Kawashima S (1997). Lesions of gonadotropin-releasing hormone-immunoreactive terminal nerve cells: effects on the reproductive behaviour of male dwarf gouramis. *Neuroendocrinology* **65**, 403–412.

Yang JJ, Wang YT, Cheng PC, Kuo YJ & Huang RC (2010). Cholinergic modulation of neuronal excitability in the rat suprachiasmatic nucleus. *J Neurophysiol* **103**, 1397–1409.

Zhang C, Bosch MA, Rick EA, Kelly MJ & Ronnekleiv OK (2009). 17Beta-estradiol regulation of T-type calcium channels in gonadotropin-releasing hormone neurons. *J Neurosci* **29**, 10552–10562.

Additional Information

Competing interests

None declared.

Author contributions

T.K., conception and design of the experiments; T.K., collection, analysis and interpretation of the electrophysiological data; H.A., collection, analysis and interpretation of confocal microscopy; T.K., H.A. and Y.O., drafting of the article or revising it critically for important intellectual content. All authors read and approved the final version.

Funding

This work was supported by Grants-in-Aid from the Japan Society for the Promotion of Science (JSPS) (22–8084) (to T.K.), Ministry of Education, Culture, Sports, Science and Technology (MEXT) (20770054) (to H.A.), JSPS (20247005), MEXT (20021012) and PROBRAIN of Japan (to Y.O.).

Acknowledgements

We are grateful to Dr Min Kyun Park, Mr Buntaro Zempo, Ms Akiko Takahashi and Ms Chie Umatani (The University of Tokyo) for technical advice. We also thank Professor Naoyuki Yamamoto (Nagoya University) for the generous gift of ChAT antibody and discussion about microscopy data. Thanks are also due to Ms Miho Kyokuwa (The University of Tokyo) for animal care.